

Classification of Free vs Substrate-bound FAD and FMN Flavoenzyme

Chia-Chun Lee, Jeffrey Lee, Catherine Zhu

Background

Flavin cofactors are redox-active coenzymes that participate in a wide range of biological processes (Figure1) when bound to proteins. Flavin is found in one of the two forms when attached to enzymes: flavin adenine dinucleotide (FAD) (Figure 2A), and flavin mononucleotide (FMN) (Figure 2B).

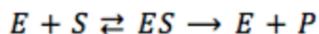


Fig. 1: Enzymatic reactions formula. E = enzymes, S = substrates, ES = enzyme/substrate complex, and p = products

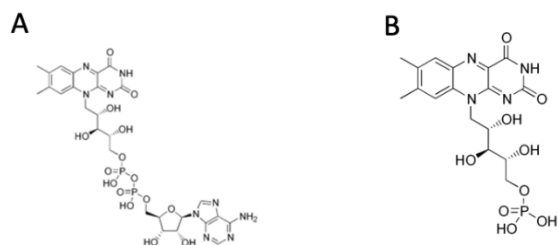


Fig. 2A: Structure of flavin adenine dinucleotide (FAD); 2B: Structure of flavin mononucleotide (FMN).

Flavin groups in FAD and FMN flavoenzymes have different structures, hence different absorption spectrum (Figure 3). Both FAD and FMN flavoproteins have two peaks between 300 nm - 500 nm, but the positions of the peaks were slightly different and therefore, it is difficult to distinguish between the two types of flavoproteins. Furthermore, the absorption spectrum is different when the flavoenzyme is free or interacting with the substrate (Figure 4). In this experiment (Figure 4), the single peak around 450 nm was shifted to 480 nm and generated a valley (convex shape) when binding to the ligand FTA. This could be due to the breaking of a Cys-8-methyl FAD bond.

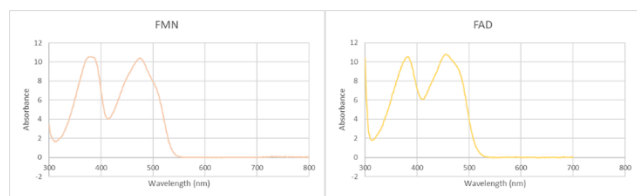


Fig. 3: Left: absorption spectra of FMN flavoenzymes; Right: absorption spectra of FAD flavoenzymes.

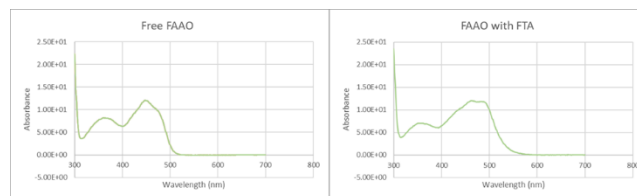


Fig. 4: Left: Free FAAO (substrate-free). Right: FAAO with a substrate, FTA. A valley appeared at around 480 nm when FTA bound to FAAO.

Upon binding to ligands, flavoenzymes change shapes and chemically modify the bound ligands, converting them to different molecule products. During the chemical reactions, molecular bonds break and form between substrates with the help of flavoproteins. The processes of chemical reactions (whether the reactions have started or finished) can be monitored by the UV absorption spectrum; however, the molecular bond transitions during the enzymatic reactions are hard to observe. For the past few years, scientists have invented methods, such as X-ray crystallography (X-ray) and Cryo-Electron microscopy (Cryo-EM), to observe molecular structures. However, these methods are not optimal to observe undergoing chemical states and the transition of molecular structures involving flavoproteins. Further, current methods are expensive and time-consuming, rendering the study of flavoproteins in bulk impossible.

Flavoenzymes play vital roles in cells, including oxidation and reductions for converting physiological signals such as cellular metabolism, light, and redox status into unique functional output. By characterizing flavoenzymes and predicting the structural changes during chemical reactions using the straight ward UV absorption spectra, we gain deeper understanding of the nature of flavoproteins and new insights of the vibrational/rotational modes of flavoproteins during chemical reactions.

The deep learning method proposed in this study attempts to:

1. Categorize FAD vs FMN flavoenzymes
2. Classify free enzymes vs enzyme/substrate complex during biological reactions based on absorption spectrum.

Through these, we hope to consistently apply a deep learning algorithm for extracted absorption curves from journals and papers to build a classifier for these flavoenzymes.

Considering the goal of the study, we wished to utilize a deep learning algorithm that could correctly classify the various types of flavoenzymes based upon the shape of the absorbance curves from research literature. Furthermore, many journals only provide spectrum plots but not complete dataset. Thus, a Convolutional Neural Network (CNN, Figure 5) was chosen, despite the sparsity of image pixels.

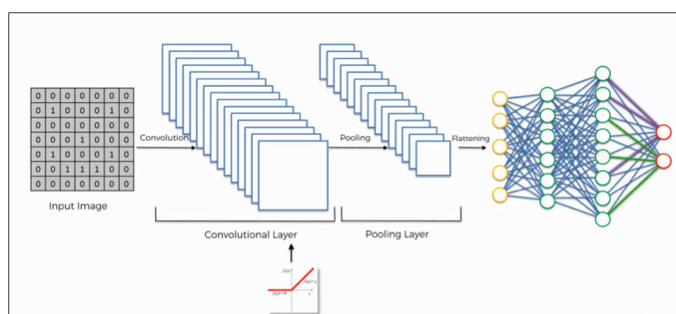


Figure 5. CNN contains convolutional layers which consist of filters to transform and process the data before feeding to the next layer. CNN uses a neural network to learn and as the number of iterations increases, the neural network can adjust based on loss functions and finally recognize patterns and features of the data .

Methods

The original data (images of flavoprotein absorbances) comes from Dr. Palfrey from the University of Michigan. Initial observations provide evidence of how indistinguishable the peaks between FAD, FMN, and substrate free/bound were. Other issues, such as inconsistent size of some images and a general lack of data samples, required processing before feeding into the CNN.

Image processing included multiple parts that addressed our concerns. Firstly, to rectify small sample size, we augmented the data by applying smooth filters on the plots using the cv2 package, which allowed for slight image blurring to increase the sample size to an acceptable level (Figure 6). Then using Imagemagick, we reshaped the images and removed the alpha channel of each of the images to obtain gray scale images of the same size. With the fully processed images, the images were hand labeled into two datasets that were our goals. The first set was the multinomial response – FAD-free,

FAD-Substrate, FMN-free, and FMN-Substrate – while the second set the binary response: FAD and FMN.



Fig. 6: Data augmentation. Smoothing filter was applied to images to increase the sample size.

The initial attempt at the 4-class model's included standard procedure for CNN's generally applied for this level of complexity. The steps were:

1. Split the dataset into a 70/30 split
2. Rescale data to binary input: $[-1, 1]$
3. Feed Forward to 3 convolutional layers and 2 dense layers
4. Kernel size: 3×3
5. Applied drop-out after first layer
6. Adam optimizer implemented with various activations.
7. Epochs = 150
8. Employ early stop
9. Validate on 30% of training set
10. Employ sparse categorical entropy loss to account for sparsity of black pixels
11. Evaluate model on test set

The architecture is shown below (Table 1).

Layer	Type	Maps	Kernel size	Activation
F9	Fully Connected	-	-	softmax
D8	Dropout	-	-	-
F7	Fully Connected	-	-	tanh
S6	Max Pooling	64	-	-
C5	Convolution	64	3×3	relu
S4	Max Pooling	36	-	-
C3	Convolution	36	3×3	relu
S2	Max Pooling	12	-	-
C1	Convolution	12	3×3	relu
In	Input	1	-	-

Table 1: The four class CNN architecture. A similar architecture for the binary model was utilized.

After implementing this model, we discovered that this network had some issues and adjusted the model by changing class weights, standardizing the dataset, and increasing the number of epochs from 150 to 5000.

As our other goal (mostly to compare model performance) is to classify between two categories of

flavoproteins, the architecture utilized was mostly the same as our initial attempt except for the binary output. The split of the data into its respective training/validation/test sets were also utilized in the same manner.

As the tuning of hyperparameters for CNN’s can be an arduous task, we utilized a tuning algorithm that performs a hyperband search over a range of various hyperparameters to expedite this process. This tuner would go through a set number of trials and then determine which combination of parameters gave the best results. The parameters from the tuner (include dropout, learning rate, initial input map) were then implemented into the architecture and its metrics monitored.

Results

Model Type	Epochs	Train Loss	Train Accuracy	Val Loss	Val Accuracy	Test Loss	Test Accuracy
4 Class	94	0.7504	0.6954	0.7212	0.7798	0.7329	0.7103
Adj. 4 Class	5000	0.8143	0.7923	0.4867	0.8214	0.5266	0.7853
2 Class	121	0.3313	0.8878	0.347	0.8698	0.3104	0.8967

Table 2: Performance metrics of the main models. The hyper parameter tuned model is not included as the performance did not truly improve.

While the hyperparameter tuner did produce outstanding results for the 2-class model, we believe that the high accuracy and abysmal loss it produced were not a realistic representation of network performance (Figure 7). Moving on to manual adjustments to the model met realistic expectations (Table 2). For the binary architecture, the validation loss crosses over and remains higher than the training loss until the number of epochs completes. Even more surprising is when using the hyperband algorithm for the four class model. The validation accuracy fluctuates heavily and the resulting testing accuracy is at an unacceptable level.

When looking at the initial four class CNN metrics (Figure 8), an interesting behavior is seen where the validation accuracy is higher than the training accuracy. Generally, this occurs with imbalanced classes, too small of a training/validation set, not using a random split for training/validation, and low variance in the data. For this study, we adjusted the model to rectify low variance and imbalanced classes. After the adjustment the CNN performance improves for both metrics; however, it must

be noted that because of the increased number of epochs, it becomes harder to ascertain whether validation accuracy truly is higher throughout the entire process and whether CNN overfits the data. The CNN architecture applied for the binary output provided outstanding results. Many factors can go into this such as the smaller number of outputs and the classes having a more balance. Manually adjusted parameters for our CNN architecture proved most realistic with favorable performance.

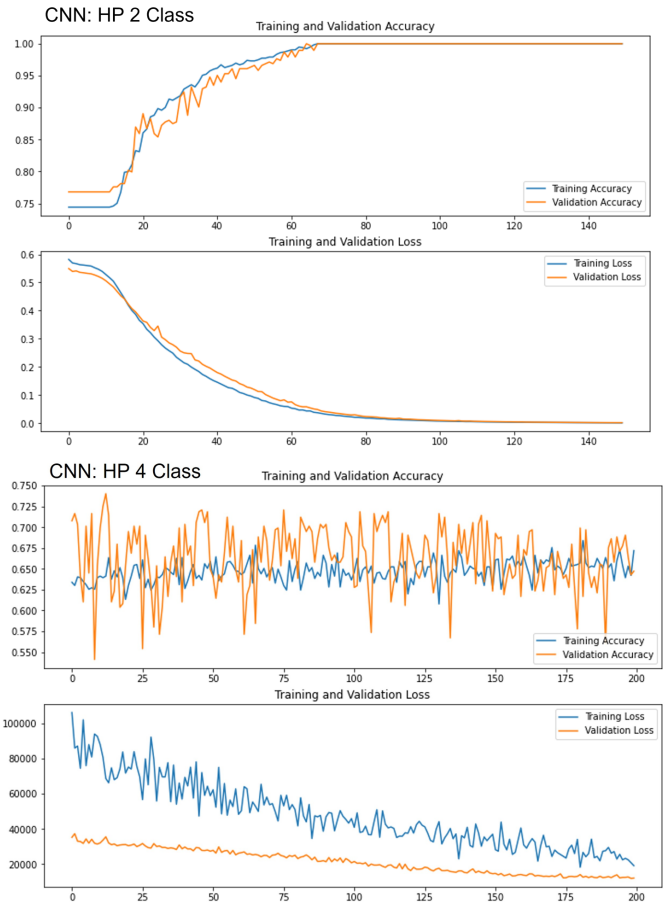


Fig. 7: Performance metrics of the 4/2 class CNNs by hyperband search method. Note that the early stop was not applied here.

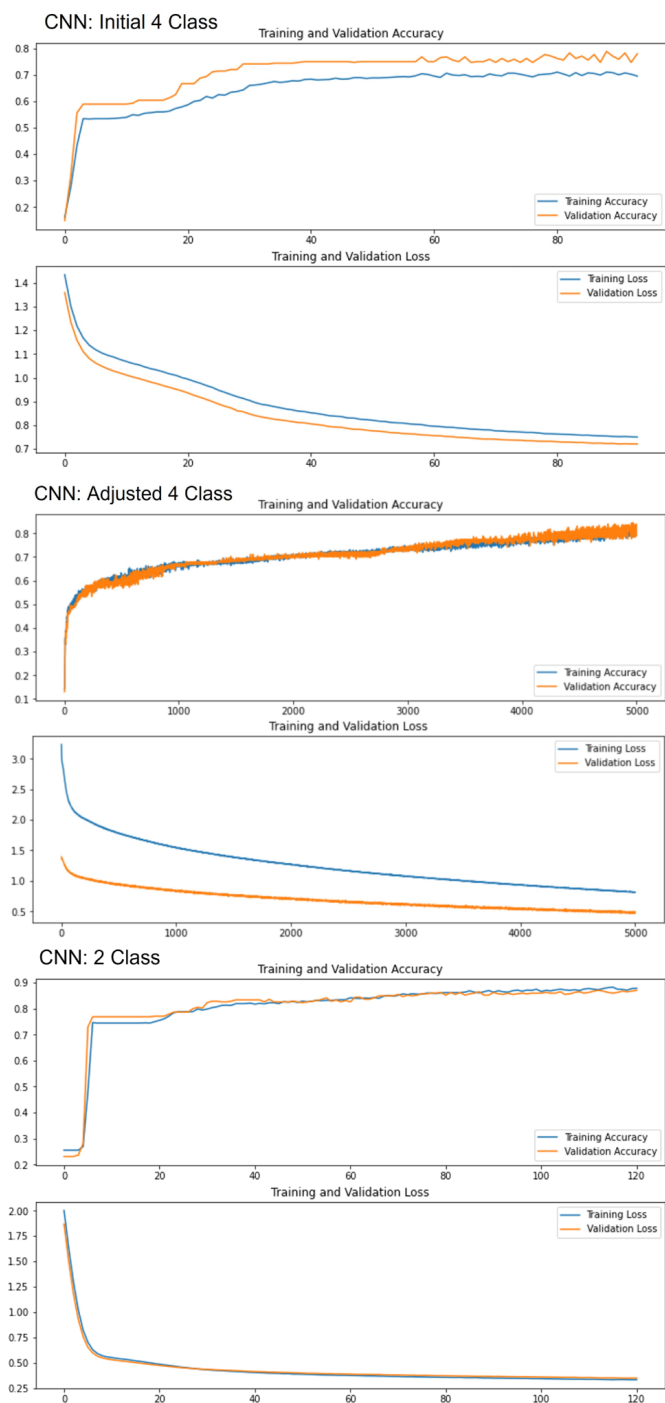


Fig. 8: Performance metrics for the 4/2 class CNN for our optimal architecture. Validation accuracy is higher than training accuracy for the initial 4 class model due to the imbalance samples between classes.

Conclusion

Overall, the Convolutional Neural Network with our current architecture performed well for our classification of flavoproteins as well as the state of these enzymes. The CNN outperformed when handling the binary output classification task when compared to the multinomial

task. We believe that the imbalanced classes present for the multinomial dataset were the main culprit for the slightly lower performance.

The hyperparameter tuner had the potential to outperform our manual tuning of the parameters; however, due to the lack of computational resources (each trial could take up to 30 minutes with GPU enabled sources) and time, the random search version did not produce fruitful results. Furthermore, it must be noted that the hyperband tuner algorithm did not aide in

Future Work

A different architecture design could help improve results for the future. First and foremost, increasing the sample size of the original dataset and not having to augment the data could greatly improve the CNN performance. Another aspect to improve upon architecture design is incorporating prior knowledge, that is to adjust the components of the model with important features by increasing their weight and decreasing the weight of unimportant ones. Finally, a different deep learning architecture could provide the most efficient results.

References

1. Becker DF, Zhu W, Moxley MA. Flavin redox switching of protein functions. *Antioxid Redox Signal*. 2011;14(6):1079-1091. doi:10.1089/ars.2010.3417
2. Schmid, Franz-Xaver. "Biological Macromolecules: UV-visible Spectrophotometry." *Encyclopedia of Life Sciences* 2005: 240-243. Web.
3. Walsh CT, Wencewicz TA. Flavoenzymes: versatile catalysts in biosynthetic pathways. *Nat Prod Rep*. 2013;30(1):175-200. doi:10.1039/c2np20069d
4. Mosegaard S, Dipace G, Bross P, Carlsen J, Gregersen N, Olsen RKJ. Riboflavin Deficiency-Implications for General Human Health and Inborn Errors of Metabolism. *Int J Mol Sci*. 2020;21(11):3847. Published 2020 May 28. doi:10.3390/ijms21113847
5. Ozsvari B, Bonuccelli G, Sanchez-Alvarez R, Foster R, Sotgia F, Lisanti MP. Targeting flavin-containing enzymes eliminates cancer stem cells (CSCs), by inhibiting mitochondrial respiration: Vitamin B2 (Riboflavin) in cancer therapy. *Aging*

(Albany NY). 2017;9(12):2610-2628.
doi:10.18632/aging.101351

6. S. Albawi, T. A. Mohammed and S. Al-Zawi, "Understanding of a convolutional neural network," 2017 International Conference on Engineering and Technology (ICET), 2017, pp. 1-6, doi: 10.1109/ICEngTechnol.2017.8308186.